Birefringence, X-ray Scattering, and Neutron Scattering Measurements of Molecular Orientation in Sheared Liquid Crystal Polymer Solutions

K. Hongladarom,[†] V. M. Ugaz,[†] D. K. Cinader,[†] W. R. Burghardt,*[,†] and J. P. Quintana[‡]

Department of Chemical Engineering and Department of Materials Science and Engineering, Northwestern University, Evanston, Illinois 60208

B. S. Hsiao

DuPont Central Research and Development, P.O. Box 80302 Wilmington, Delaware 19880

M. D. Dadmun

Department of Chemistry, University of Tennessee, Knoxville, Tennessee 37996

W. A. Hamilton and P. D. Butler

Solid State Division, Oak Ridge National Laboratory, Oak Ridge, Tennessee 37831

Received February 5, 1996; Revised Manuscript Received May 13, 1996[⊗]

ABSTRACT: Recent studies of molecular orientation in sheared liquid crystalline polymers have often yielded contradictory results. To check the self-consistency of methods for quantitative measurements of molecular orientation, liquid crystalline solutions of (hydroxypropyl)cellulose [HPC] and poly(benzyl glutamate) [PBG] have been studied using flow birefringence, X-ray scattering, and neutron scattering. HPC X-ray scattering patterns show an arclike pattern with a distinct peak as a function of scattering vector, while PBG patterns show a more diffuse equitorial streak. These differences are attributed to more strongly correlated lateral packing in HPC solutions due to their higher concentration. Measurements of orientation in steady shear flow agree well among the three techniques. Lyotropic HPC and PBG solutions differ in orientation at low shear rates. HPC solutions exhibit near zero orientation at low rates, while X-ray and neutron scattering measurements confirm previous birefringence data showing a low shear rate plateau of moderate orientation in PBG. Differences with recent neutron scattering measurements on PBG solutions that show low orientation at low shear rate are attributed to choice of solvent, rather than choice of technique. X-ray and optical data are consistent in showing decreasing orientation in HPC solutions during relaxation, but discrepancies are found in relaxation of PBG solutions. Large increases in flow birefringence suggest substantial orientation enhancement. X-ray data on one PBG solution confirm increasing orientation, but X-ray and neutron scattering data on a more concentrated solution show only modest changes in orientation. It is suggested that flow birefringence fails in this case due to texture coarsening to the point where there is no longer effective averaging over the distribution of director orientations along the light path.

1. Introduction

Improved understanding of the relationship between applied flow and molecular orientation in liquid crystalline polymers (LCPs) yields insights into processing operations where flow-induced orientation influences product properties, as well as the unusual rheological behavior exhibited by LCPs. Toward this end, the past five years have seen numerous studies reporting quantitative measurements of orientation in LCP solutions under flow, using several techniques. Most of this effort has concentrated on lyotropic solutions of rodlike polymers in simple shear flow. Despite improved understanding of the molecular origins of complex rheology in LCP solutions,[1] many phenomena are not universally observed. Similarly, measurements of shear-induced orientation in LCPs reveal a wide range of behavior. Since these studies have employed different combinations of techniques and model systems, it is not clear to what extent differences may reflect inconsistencies between methods as opposed to variations in behavior of different materials. The goal of this work is to compare molecular orientation measured using *multiple* methods on several different model LCP solutions, to identify the extent to which different techniques provide self-consistent results.

Techniques used in recent years to characterize molecular orientation in LCP solutions under flow include X-ray scattering,[2−7] UV dichroism,[8] birefringence,[9−14] and small-angle neutron scattering.[15−17] Scattering methods are based on the fundamental anisotropic shape of rodlike molecules: an anisotropic distribution of molecular orientation leads directly to an anisotropic scattering pattern. Dichroism and birefringence measurements are sensitive to anisotropy in refractive index, resulting from anisotropic dielectric properties at the molecular level averaged on length scales comparable to the wavelength of light over the local distribution of molecular orientation.

All measurements of molecular orientation in LCPs must be interpreted in light of their usually *textured* morphology. LCPs spontaneously order at the molecular level, with a degree of alignment characterized by

* Author to whom correspondence should be addressed (w-burghardt@nwu.edu).
[†] Department of Chemical Engineering, Northwestern University.
[‡] Department of Materials Science and Engineering, Northwestern University.
[⊗] Abstract published in *Advance ACS Abstracts,* July 1, 1996.

a molecular order parameter S_m, which has an equilibrium value S^{eq}. However, LCPs typically exhibit a proliferation of orientational defects (disclinations) that tend to disrupt orientation on length scales of 1 to 10 μm. It is thus necessary to admit the presence of a distribution of *director* orientations (often conceptualized as a distribution of "domain" orientations in analogy to polycrystalline solids). These effects have often been accounted for through the use of a texture or mesoscopic order parameter, $\bar{S}$.[3,9,18,19] For example, a quiescent LCP is often envisioned with $\bar{S} = 0$, so that there is no *macroscopic* orientation despite the spontaneous ordering at the molecular level.

The application of an external field can influence orientation at both the molecular and mesoscopic level. Under these circumstances, macroscopic measurements of molecular orientation in LCP solutions will be influenced by both levels of structure:

$$S = \bar{S} S_m \tag{1}$$

This interpretation of bulk orientation measurements has been widely used and is of great conceptual value. However, since flow can affect both molecular and mesoscopic order parameters, it is difficult to precisely unravel the relative contributions to measured flow-induced orientation. In addition, order parameters are properly thought of as tensorial quantities under flow, of which certain projections are sampled.[9] Further, the orientation distributions (both molecular and mesoscopic) need not be uniaxial under flow.[12] However, for the case of uniaxial distributions of orientation (appropriate, for instance, in alignment by a weak magnetic field where the molecular orientation distribution is not perturbed), Walker and Wagner have demonstrated that the product embodied in eq 1 is rigorously valid in interpreting scattering data.[19]

Since scattering patterns are built up essentially one molecule at a time, the distribution of scattered intensity naturally reflects both the distribution of director orientation in space and the distribution of molecular orientation about the director simultaneously. The situation for optical methods such as birefringence is somewhat less clean. As a polarized light beam passes through a sample, its polarization state continually evolves as a result of its interaction with the anisotropic refractive index tensor. The cumulative effect of these changes are analyzed in the light beam that exits the sample. Locally, the birefringence experienced by the light is determined by the *molecular* orientation state, since "domain" sizes are typically larger than the wavelength of light. Provided that the texture is small compared to the light path, however, a large number of domains will be sampled as the light passes through the sample, this being the mechanism by which the distribution of domain orientations is averaged in the bulk birefringence measurement. Variations in averaged properties from one light path to another lead to a gradual mixing of the polarization state, which, although potentially useful for studying texture sizes under flow,[20] can interfere with birefringence measurements.[9,10] From these considerations, it is clear that scattering methods should provide a more direct measure of bulk orientation. At the same time, birefringence offers substantial advantages with respect to convenience and cost, particularly when transient measurements are desired.

The studies cited above have given varying results for the behavior of LCP molecular orientation in shear flow. Picken and co-workers observed a high degree of orientation in polyaramid solutions at all shear rates studied using X-ray scattering.[2,3] Chow and co-workers found near zero orientation in solutions of PBZT at low shear rates and moderate degrees of orientation at higher rates.[8] In poly(benzyl glutamate) [PBG], birefringence studies by Hongladarom *et al.* showed two distinct regimes in orientation: a low shear rate plateau with moderate orientation, followed by a transition to high orientation at high rates.[9] However, Dadmun and Han[15] observed an additional transition to near zero orientation at low rates using neutron scattering on PBG solutions of similar concentration, but with a different solvent. Low orientation at low rates in PBG was also seen with neutron scattering by Walker[21] in yet another solvent and at higher polymer concentration than that studied by Hongladarom *et al.* Studies on various solutions of (hydroxypropyl)cellulose [HPC] by X-ray[4,5] or neutron[17] scattering as well as birefringence[11,13] generally show near zero orientation at low shear rates, with transitions to increasing orientation with increasing shear rate. In light of these differing results for different techniques and samples, particularly in the case of PBG where only the solvent is different, our goal here is to provide the first comprehensive comparison of these different methods for measuring molecular orientation.

2. Experimental Methods

2.1. Materials. Several model lyotropic LCP solutions have been studied. HPC solutions in water and *m*-cresol have been studied by birefringence and X-ray scattering. The aqueous solution has a concentration of 50 wt % ($c = 0.542$ g/mL), with a nominal polymer molecular weight of 60000 (Klucel E from Hercules). Rheology and molecular orientation in this solution were studied extensively by Hongladarom *et al.*[11] Recent work by Guido and Grizzuiti[22] suggests that 50 wt % HPC is likely to be biphasic; however, its rheology appears to be dominated by the liquid crystalline phase. The *m*-cresol solution has a concentration of 27 wt % ($c = 0.289$ g/mL) and was prepared from a different lot of Klucel E. This solution has been previously studied in both simple shear[13] and complex flows[23] using flow birefringence.

Studies were also performed on solutions of poly(benzyl glutamate) in *m*-cresol. We have performed X-ray measurements on a 13.5 wt % ($c = 0.143$ g/mL) solution of the single optical isomer PBDG with reported molecular weight 298000 studied previously by Hongladarom and Burghardt using multiple birefringence techniques.[12] Finally, we have studied a pair of more concentrated solutions of PBLG (molecular weight 318000) in *m*-cresol. For birefringence and X-ray scattering studies, a 19 wt % ($c = 0.204$ g/mL) solution was prepared in normal *m*-cresol. For neutron scattering studies, a corresponding solution was made in deuterated solvent, *m*-cresol-d_8, purchased from CDN Isotopes. This solution had a polymer concentration of 18 wt %, to give it the same volume fraction as the 19 wt % solution studied with birefringence and X-ray scattering. PBG samples and *m*-cresol were purchased from Sigma.

Lyotropic solutions of HPC and single optical isomers (L or D) of PBG are cholesteric at rest. It is usually assumed that cholesteric LCP solutions transform to the nematic phase under shear. In the case of PBG, racemic mixtures containing equal amounts of L and D isomers may be prepared, which are nematic in the quiescent state. Previous measurements have to date shown no significant differences in either structural or rheological behavior between racemic PBG solutions and solutions of single isomers,[9,10] suggesting that cholestericity in PBLG or PBDG does not affect the flow behavior. However, it has been postulated that HPC rheology may be influenced by persistence of cholestericity at low shear rates.[11]

HPC and PBG solutions are useful model systems in that they exhibit clear rheological signatures of transitions from

tumbling dynamics at low shear rates to flow alignment at high shear rates, so that orientation behavior may be compared with predictions of molecular rheological models. Much of our previous work has explored the relationship between bulk molecular orientation and shear rheology in detail.[9−11,13] Here we concentrate on measurements of fluid structure. All steady state and relaxation measurements were taken after the sample had been sheared for 200 or more strain units.

2.2. Flow Birefringence Measurements. Birefringence measurements were carried out in a rotating parallel disk flow cell constructed from optical windows, using a spectrographic birefringence technique. The light beam passes along the shear gradient axis, displaced sufficiently far away from the rotation axis of the flow cell that the shear rate is nearly uniform. Orientation is thus probed in the flow-vorticity plane. A computer-controlled stepping motor was used to drive the flow at the desired shear rate. Details about the experimental equipment and methods may be found elsewhere.[9,10]

2.3. X-ray Scattering Measurements. X-ray scattering experiments were performed at beamline X18A at the National Synchrotron Light Source at Brookhaven National Laboratory. Focused, monochromatic bending magnet radiation had energy of 7 keV, corresponding to a wavelength of 1.77 Å. The flow cell used for birefringence measurements was modified for X-ray scattering experiments by replacing the optical glass windows with thin sheets of mica supported on steel or aluminum plates through which holes were cut to allow X-ray transmission. On the rotating plate, these took the form of three slits arranged circumferentially, following the design of Keates et al.[5] This configuration allows X-ray transmission over roughly 85% of the flow cell rotation. To enable operation with the rotation axis horizontal, the modified flow cell also incorporates a Teflon bearing seal. The horizontal X-ray beam again passes parallel to the shear gradient axis. The flow cell was followed by helium-filled chambers of various lengths to reduce air scattering. Lead beam stops were located roughly half way along the length of the helium chambers. Two-dimensional scattering patterns were collected and digitized using Fuji image plates and scanner, and the image plate intensity was converted to a linear scale for subsequent analysis. Images were further normalized by measurements of incident beam intensity collected simultaneously with the exposure, and, if necessary, corrected for the transient interruptions of the beam by the rotating flow cell.

Transient relaxation data were obtained by exposures on successive image plates. In order to improve temporal resolution, relaxation experiments were repeated with interleafed exposure schedules.

2.4. Neutron Scattering Measurements. Small angle neutron scattering measurements were performed on the 30 m SANS instrument at the High Flux Isotope Reactor in Oak Ridge National Laboratory. Detailed descriptions of the instrument and calibration procedures may be found elsewhere.[24,25] A wavelength of 4.75 Å was used. The incident beam was collimated using beam guides and passed through a quartz Couette shear cell. The shear cell was positioned such that the beam passed through the flow cell along its diameter, and thus the beam was again directed along the velocity gradient direction. At higher shear rates, the fluid−air interface became uneven around the flow cell circumference due to imperfections in the shear cell. This limited shear rates to 35 s^{-1} and below for the neutron scattering experiments. Scattered neutrons were collected by a 64 × 64 cm^2 area detector which was placed at a sample to detector distance of 2.3 m. The collected scatterng data were corrected for empty cell scattering, detector nonlinearity, electronic noise and stray scattering, sample transmission, and background incoherent scattering. The data were then reduced to absolute differential scattering cross section (in cm^{-1}) using water as a secondary standard.

In both neutron and X-ray scattering measurements, intensity is reported as a function of azimuthal angle ϕ measured from the flow direction, and scattering vector, $q = 4\pi \sin(\theta/2)/\lambda$. Here θ is defined as the angle between the incident and scattered radiation. Note that this definition of scattering angle is consistent with common usage in neutron scattering,[26] but departs from conventions commonly used in X-ray scattering.[27]

3. Results

3.1. Scattering Patterns. Figure 1 shows representative 2-D X-ray scattering patterns for the four solutions studied under shear, and a typical neutron scattering pattern for the PBLG solution in deuterated cresol. At this shear rate, all solutions exhibit a moderate degree of flow-induced orientation, leading to pronounced azimuthal dependence of the scattered intensity. Figure 2 shows radial scans of the scattering patterns taken perpendicular to the flow direction (azimuthal angle $\phi = 90°$). The HPC solutions show a pronounced peak in scattered intensity at scattering vector q^*. This peak is generally attributed to strongly correlated lateral packing of rodlike molecules in plane perpendicular to the director. The more highly concentrated aqueous solution exhibits a shorter correlation length ($d \approx 2\pi/q^* = 13$ Å) than the *m*-cresol solution ($d \approx 19$ Å). The PBG solutions have lower concentration, and exhibit correspondingly weaker signs of correlation in lateral packing, with humps in scattered intensity as a function of q. The correlation length may be estimated for the 19 wt % PBLG solution ($d \approx 23$ Å), but the correlation peak is too diffuse in the 13.5 wt % solution to estimate a length scale with any confidence. Varying shear rate changes the azimuthal distribution of scattered intensity, but the shape and location of the correlation peaks do not change with shear rate.

Comparison of X-ray and neutron scattering patterns in the matched PBLG solutions, Figure 1d,e, shows them to be qualitatively similar. Due to the longer wavelength, neutron scattering probes structure at longer length scales (smaller q). However, the radial scans appear to exhibit the same general decrease in scattered intensity with scattering vector for both X-ray and neutron scattering. Since we are unable to convert X-ray scattering to an absolute scale, direct quantitative comparison is not possible; nevertheless, it is clear that these two techniques provide complementary information about the same underlying structure at different length scales.

3.2. Analysis Procedures. Scattering measurements of orientation in LCP solutions have often drawn analogy to similar measurements of orientation in polycrystalline solids with a uniaxial bias in orientation (such as in drawn fibers of semicrystalline polymers). In a single crystal, reflections are located at discrete points in reciprocal space. A distribution of crystallite orientations leads to spreading of these points on spherical surfaces in reciprocal space; measurement of the degree of spreading of diffracted intensity thus provides a measure of the degree of crystallite misalignment.[27] The analogy is imperfect in nematic LCP solutions, since they possess only liquidlike structure at small length scales and thus no sharp reflections. In most cases, the correlation peak associated with lateral packing of chains has been chosen as the "reflection", and an orientation parameter is extracted from an azimuthal scan of scattered intensity at the peak scattering vector q^*. While this seems quite appropriate when the correlation peak is strong, as in Figure 2a, the polycrystalline outlook becomes less satisfying when spatial correlations are less strong, as in Figure 2b. Further, while the neutron scattering pattern clearly reflects molecular orientation, its range of scattering vector is outside of any pseudocrystalline "reflection".

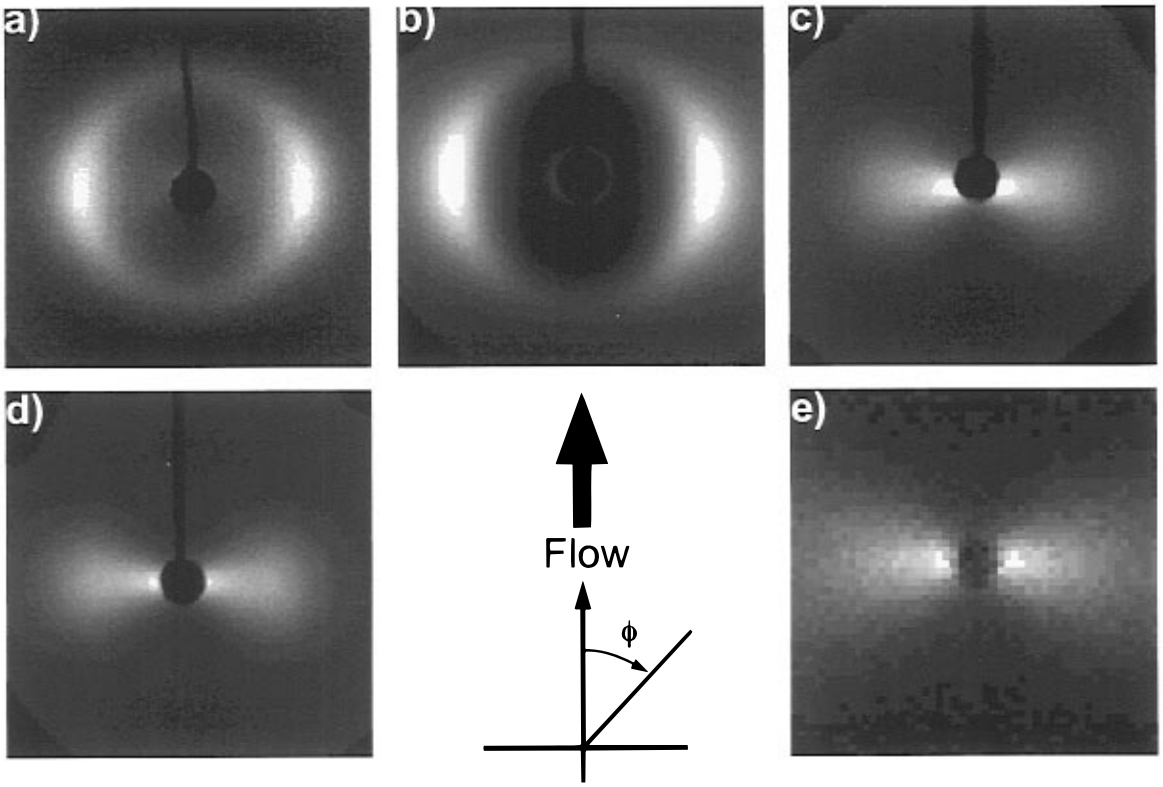

Figure 1. Two-dimensional scattering patterns for LCP solutions sheared at 2 s^{-1}. (a) X-ray pattern for 50 wt % HPC in water; $q = 0.765$ Å^{-1} at pattern half-width. (b) X-ray pattern for 27 wt % HPC in *m*-cresol; $q = 0.465$ Å^{-1} at pattern half-width. (c) X-ray pattern for 13.5 wt % PBDG in *m*-cresol; $q = 0.502$ Å^{-1} at pattern half-width. (d) X-ray pattern for 19 wt % PBLG in *m*-cresol; $q = 0.502$ Å^{-1} at pattern half-width. (e) Neutron scattering pattern for 18 wt % PBLG in *m*-cresol-d_8; $q = 0.154$ Å^{-1} at pattern half-width. Gray scales adjusted to give good contrast for each image.

Walker and Wagner[19] have modeled neutron scattering patterns in PBG solutions simply as a convolution of the highly anisotropic form factor for rods with the orientation distribution function of the rodlike macromolecules, a description which is also appropriate for X-ray scattering.[28] For an *infinite* rod, scattered intensity in reciprocal space is confined to an infinitely narrow plane normal to the rod axis. An azimuthal scan of intensity scattered from the rod would thus be a δ function: a single infinite rod is analogous to a crystallite in the former approach. The influence of finite molecular length in experiments depends on the magnitude of the scattering vector. Following Walker and Wagner,[19] consider the form factor for an individual rod of finite length L:

$$F(\mathbf{q},\mathbf{u}) = \sin(\mathbf{q}\cdot\mathbf{u}L/2)/(\mathbf{q}\cdot\mathbf{u}L/2) \qquad (2)$$

where $\mathbf{q}$ is the scattering vector, $\mathbf{u}$ is a unit vector along the rod axis, and L is the rod length. For PBG of molecular weight 300000, $L \approx 2050$ Å. Figure 3 illustrates the azimuthal dependence of the form factor for a single aligned molecule for values of q typical of both neutron and X-ray experiments. Due to finite length, the scattering is less well confined to the normal plane, leading to azimuthal spreading that is more severe at the smaller scattering vectors probed in neutron scattering.

The applicability of the "polycrystalline" approach depends directly on how faithfully this distribution approximates a δ function. Since X-rays naturally probe shorter length scales, the effect of finite rod length becomes minimal at larger q. For our X-ray measurements, we directly apply the approach outlined by Mitchell and Windle and Keates and co-workers.[4,5] Molecular orientation is characterized in terms of the azimuthal intensity averages of the second spherical harmonic component of a uniaxial distribution function, $P_2(\cos\phi) = (1/2)(3\cos^2\phi - 1)$. The orientation parameter, S, is calculated by:

$$S = \frac{\langle P_2(\cos\phi)\rangle_{\text{sample}}}{\langle P_2(\cos\phi)\rangle_{\text{o}}} \qquad (3)$$

The brackets indicate averaging over an azimuthal intensity scan:

$$\langle P_2(\cos\phi)\rangle = \frac{\int_0^{\pi/2} I(q,\phi)P_2(\cos\phi)\sin\phi\,\mathrm{d}\phi}{\int_0^{\pi/2} I(q,\phi)\sin\phi\,\mathrm{d}\phi} \qquad (4)$$

and $\langle P_2(\cos\phi)\rangle_{\text{o}} = -1/2$ is the value that would be observed if all rods were perfectly aligned. To be consistent with others, we used $q = q^*$ for this analysis, since intensity is concentrated at this scattering vector due to the local packing structure of the molecules. At the smaller q values (and hence larger length scales) probed by neutron scattering, there will be more significant azimuthal spreading of intensity from a single aligned rod. To extract a measure of orientation, one option is application of eqs 3 and 4, with the understanding that the additional broadening of the scattered intensity distribution will reduce the measured orientation parameter somewhat. Walker and Wagner suggested an alternate approach, where anisotropy in the scattering pattern is characterized by an "alignment factor":

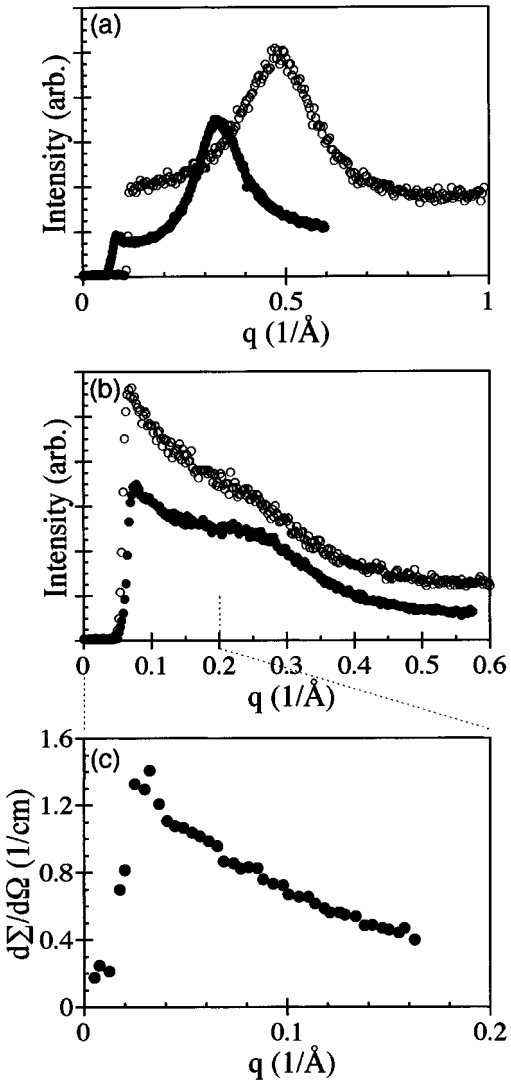

Figure 2. Radial scan of scattered intensity as a function of scattering vector at azimuthal angle $\phi = 90°$. (a) 50 wt % HPC in water (○) and 27 wt % HPC in *m*-cresol (●), X-ray scattering. (b) 13.5 wt % PBDG in *m*-cresol (○) and 19 wt % PBLG in *m*-cresol (●), X-ray scattering (c) 18 wt % PBLG in *m*-cresol-d_8, neutron scattering. Data in a and b represent single pixel width slices of X-ray scattering images, while the neutron data in c were averaged over a range of azimuthal angle $80° < \phi < 100°$.

$$A_f(q) = \frac{\int_0^{\pi/2} I(q,\phi)\cos(2\phi)\, d\phi}{\int_0^{\pi/2} I(q,\phi)\, d\phi} \qquad (5)$$

whose value ranges from zero for an isotropic scattering distribution to −1 for the case when scattering is concentrated solely at $\phi = 90°$. Walker and Wagner then compared experimental measurements of $A_f(q)$ with values calculated by convolving a uniaxial distribution function of known order parameter with the finite rod form factor.[19] Alternatively, A_f itself may be taken as a measure of molecular orientation.[16] Dadmun and Han[15] characterized anisotropy in scattering patterns in terms of the peak heights and widths of azimuthal intensity scans such as those presented in Figure 4b, having fit the peaks with a Lorentzian curve.

Figure 4a shows typical X-ray azimuthal intensity scans for steady shear flow of the PBLG solution. Even at the lowest shear rates studied, the scattering patterns for PBLG are quite anisotropic, indicative of a significant degree of flow-induced molecular orientation. With increasing shear rate, scattering along the flow direction ($\phi = 0°$) is suppressed, while scattering in the equatorial direction ($\phi = 90°$) increases, indicative of increasing orientation. At the highest shear rates, the scattering peaks become narrower and higher, but with little change in the scattered intensity along the flow direction. This suggests that there is no longer a significant population of molecules oriented perpendicular to the flow direction. The remaining intensity presumably reflects parasitic effects such as scattering from solvent, air, and the flow cell. Following the suggestion of Mitchell and Windle,[28] we take the lowest scattering value observed at $\phi = 0°$ at the highest shear rates for each sample as a base line value for analyses according to eqs 3 and 4.

Figure 4b shows analogous azimuthal scans from neutron scattering experiments on the matched solution in deuterated solvent. The degree of anisotropy is

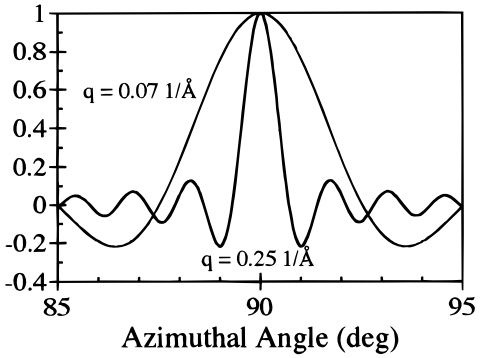

Figure 3. Calculated azimuthal dependence of form factor for a perfectly aligned rod of finite length $L = 2050$ Å. Curves drawn using eq 2, with $q = 0.07$ and 0.25 Å^{-1}, characteristic of neutron and X-ray experiments, respectively.

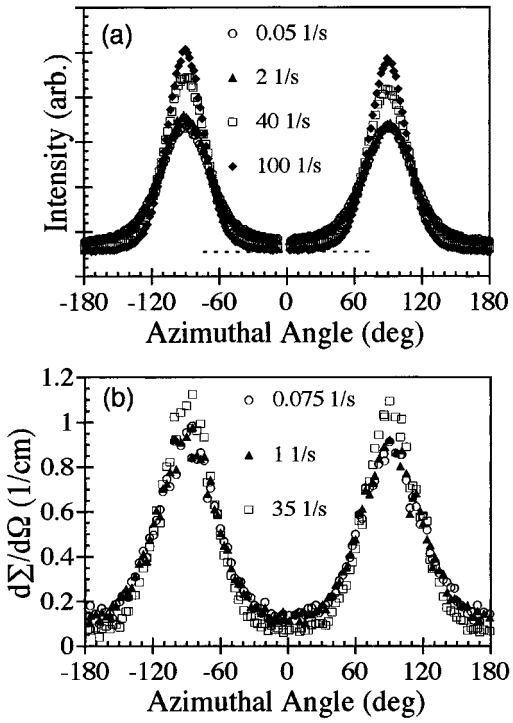

Figure 4. Typical azimuthal scans of scattered intensity. (a) 19 wt % PBLG in *m*-cresol, scans taken at $q = 0.268$ Å^{-1}, for X-ray scattering at indicated shear rate. Dashed line indicates base line chosen for subsequent order parameter analysis. (b) 18 wt % PBLG in *m*-cresol, scans averaged over the range $0.06 < q < 0.08$ Å^{-1}, for neutron scattering at indicated shear rate.

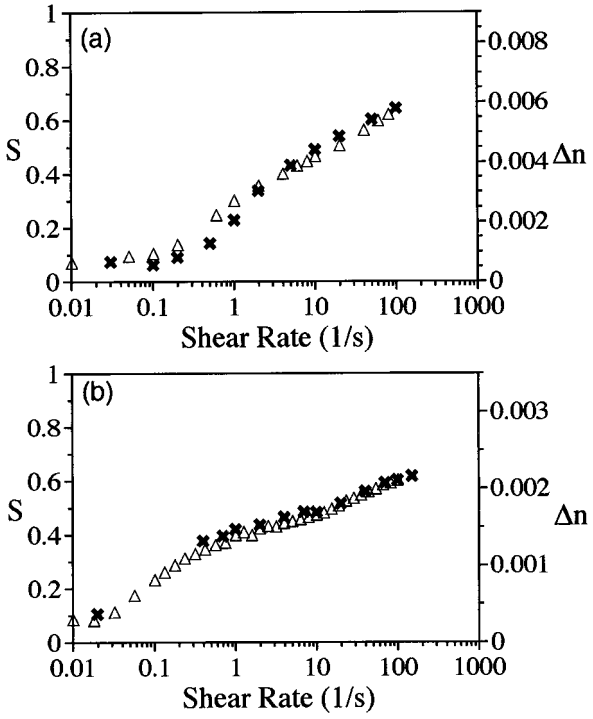

Figure 5. Molecular orientation of HPC solutions in steady shear. X-ray orientation parameter (×) and flow birefringence (Δ) as a function of shear rate for (a) 50 wt % HPC in water, and (b) 27 wt % HPC in *m*-cresol.

somewhat lower than in the X-ray patterns, consistent with greater azimuthal spreading of the rod form factor at smaller q. Over the shear rate range studied, there are modest increases in peak scattering at $\phi = 90°$ and corresponding decreases in scattering along the flow direction.

3.3. Steady State Results. Figure 5 presents flow birefringence and orientation parameter (measured by X-ray) for the two HPC solutions in steady shear flow. The scales of the birefringence axes have been adjusted in an attempt to superimpose these two measurements of orientation, since both should reflect the second moment of the orientation distribution function. X-ray data are in excellent agreement with birefringence data. Both solutions show low orientation at low rates, with transitions to higher orientation as shear rate is increased. Particularly in the case of 27 wt % HPC in *m*-cresol, there appear to be two transitions in orientation. The higher shear rate transition is well correlated with changes in sign of the first normal stress difference and thus presumably reflects the transition from tumbling to flow aligning dynamics.[13] The low orientation observed at the lowest shear rates appears concurrently with so-called "Region I" shear thinning,[11,13] suggesting that flow is unable to impart significant molecular orientation due to the dominance of distortional elastic effects associated with texture.[29]

Figure 6 presents similar results for the PBG solutions. As anticipated from anisotropy in scattering patterns at low shear rates (Figure 4), both of these solutions exhibit substantial molecular orientation at low rates, unlike HPC. Consistent with the notion that Region I shear thinning accompanies a piled polydomain structure with low orientation, PBG solutions in this concentration range also do *not* exhibit Region I shear thinning.[9,30,31] PBG solutions exhibit a transition to a higher orientation state at higher shear rates. Comparison with normal stress behavior demonstrates that this increase in orientation reflects a transition from tumbling to flow aligning dynamics.[9]

The more concentrated PBG solution was also studied by neutron scattering. Figure 6c shows orientation as

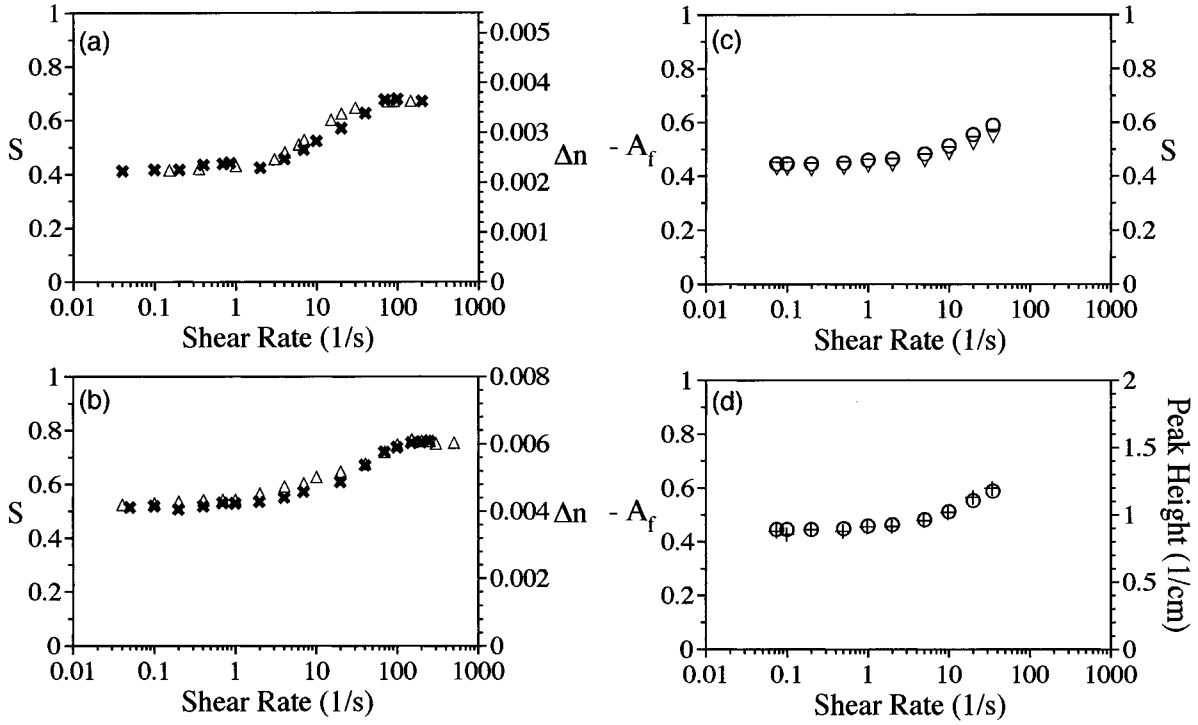

Figure 6. Molecular orientation of PBG solutions in steady shear. X-ray orientation parameter (×) and flow birefringence (Δ) as a function of shear rate for (a) 13.5 wt % PBDG in *m*-cresol, and (b) 19 wt % PBLG in *m*-cresol. (c) Alignment factor (○) and orientation parameter (▽) from neutron scattering as a function of shear rate for 18 wt % PBLG in *m*-cresol-d_8. (d) Alignment factor (○) and peak height of azimuthal intensity scan (+) from neutron scattering as a function of shear rate for 18 wt % PBLG in *m*-cresol-d_8. Neutron alignment factor and orientation parameter are based on azimuthal scans averaged over the range $0.06 < q < 0.08$ Å^{-1}.

a function of steady shear rate, characterized by alignment factor (plotted as $-A_f$) and orientation parameter calculated from azimuthal scans of neutron scattering intensity in the range $0.06 < q < 0.08$ Å^{-1}. These two measures of orientation are quite similar, which is not surprising since $-A_f$ and S both range from 0 to 1 as the scattering pattern changes from isotropy to perfect alignment. Similar agreement was reported by Walker and Wagner.[16]

Dadmun and Han used the peak height of azimuthal intensity scans to characterized changes in molecular orientation with steady shear rate. Figure 6d presents a comparison of alignment factor and peak height calculated from azimuthal scans of neutron scattering patterns for the more concentrated PBLG solution. Evidentally, both approaches provide comparable information in characterizing anisotropy in the neutron scattering pattern.

Comparing Figures 6, parts b−d, there is qualitative consistency among all three techniques for measuring orientation. In particular, the neutron scattering data also show significant molecular orientation at the lowest rates. This agrees with published birefringence data,[9] but is inconsistent with neutron scattering data of Dadmun and Han[15] and Walker[21] on other PBG solutions showing low orientation at low rates. Figure 6 shows that these discrepencies must be due to differences in solvent, and perhaps concentration, but not due to inconsistencies among the techniques used or the way in which orientation is inferred from neutron scattering patterns. Focusing on the scattering results, orientation parameters calculated from the X-ray experiments are somewhat higher than those calculated from neutron scattering. For instance, the average orientation parameters seen at low rates in Figures 6, parts b and c, are 0.515 and 0.428, respectively. This trend is expected, given the greater azimuthal broadening at smaller q in neutron measurements (Figure 3). If a similar analysis of neutron data is performed at larger scattering angle ($0.11 < q < 0.13$ Å^{-1}), a low shear rate value of 0.469 is obtained. Walker and Wagner[16] suggest that the "true" orientation parameter may be obtained by extrapolation as $q \rightarrow \infty$, since there should be less broadening at higher q according to eq 2. However, since there are significant changes in orientation measurements obtained within the q range accessible by neutron scattering, such an extrapolation would best be carried out in the context of a particular model for the orientation distribution (for instance, Walker and Wagner use the Maier−Saupe distribution). Since X-ray scattering provides data at higher q than neutron scattering, it is expected that the X-ray value should provide the best estimate of the "true" orientation parameter. At the same time, Mitchell and Windle have recognized some arbitrariness in base line subtraction procedures in X-ray measurements, which directly influence S measurements;[28] there is thus always likely to be some uncertainty in the precise significance of orientation parameters calculated in this way.

3.4. Relaxation Results. Figure 7 shows results for relaxation of orientation in HPC solutions following cessation of shear flow. In each of these solutions, orientation ultimately relaxes toward a low orientation state, accompanied by significant changes in dynamic modulus.[11,13] The scalings of birefringence axes are the same as in Figure 5; again, there is excellent agreement between optical and X-ray measurements of orientation.

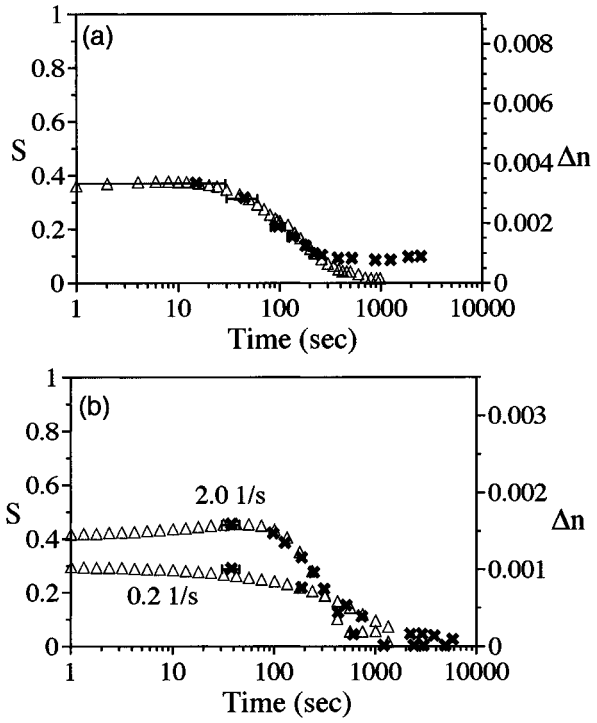

Figure 7. Relaxation of molecular orientation in HPC solutions. X-ray orientation parameter (×) and birefringence (Δ) as a function of time following flow cessation. (a) 50 wt % HPC in water; previous shear rate = 5 s^{-1}. (b) 27 wt % HPC in *m*-cresol; previous shear rates = 0.2 and 2.0 s^{-1}. Horizontal error bars on X-ray data indicate image plate exposure time.

Figure 8 presents results of similar experiments on the PBG solutions. These data are plotted as a function of time scaled by previous shear rate, in light of a ubiquitous relaxation scaling law in PBG.[10,32,33] Earlier birefringence studies established the unexpected result that molecular orientation *increases* during relaxation of PBG solutions from low prior shear rates. This provides a satisfying explanation for prior observations of decreases in dynamic modulus during relaxation.[32,33] More recently, Walker and Wagner have reported comparable increases in orientation in a different PBG solution, measured by neutron scattering.[16] Figure 8a shows consistency between X-ray and birefringence data showing increasing orientation in the 13.5 wt % PBDG solution, in agreement with these previous studies.

Surprisingly, self-consistency is *not* seen in the more highly concentrated PBLG solution. While the birefringence data in Figure 8b are similar to those in Figure 8a, X-ray and neutron scattering results do not show the strong increase in orientation suggested by the birefringence. Rather, both scattering methods show an initial increase in orientation, followed by a slight decrease in orientation, followed in turn by increasing orientation at longer times. These changes, while subtle, are seen in both X-ray and neutron scattering and show typical scaling when data for different prior shear rate are plotted against scaled time. As discussed in the introduction, scattering methods are more directly sensitive to the distribution of molecular orientation than birefringence. The self-consistency between the neutron and X-ray scattering results for the PBLG solution leaves little doubt that they reflect the true evolution of bulk molecular orientation during relaxation. Despite excellent agreement in steady shear and other relaxation experiments, birefringence fails to capture the bulk orientation in this case. Possible

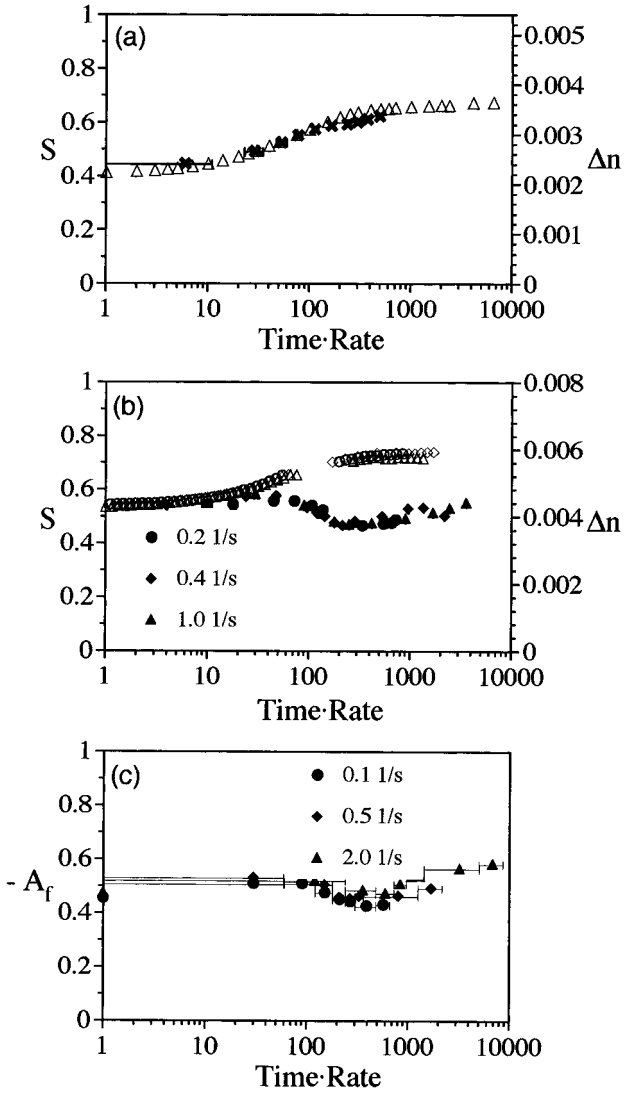

Figure 8. Relaxation of molecular orientation in PBG solutions. (a) X-ray orientation parameter (×) and flow birefringence (Δ) as a function of time multiplied by previous shear rate, for 13.5 wt % PBDG in *m*-cresol with previous shear rate = 0.2 s^{-1}. (b) X-ray orientation parameter and birefringence as a function of scaled time for 19 wt % PBLG in *m*-cresol, at indicated previous shear rates. Filled and unfilled symbols represent X-ray scattering and birefringence data, respectively. (c) Neutron scattering alignment factor as a function of scaled time for 18 wt % PBLG in *m*-cresol-d_8, at indicated previous shear rate. Symbols on absissa indicate steady state alignment factor.

causes for this failure will be discussed in the following section.

4. Discussion

We first discuss the steady shear results in which birefringence and scattering methods give self-consistent measures of molecular orientation. The ability to closely superimpose birefringence and orientation parameter through suitable selection of axis scales in Figures 5 and 6 supports the arguments of Hongladarom et al.[9] that birefringence in textured LCPs should provide a meaningful measure of bulk orientation, averaged over molecular and texture levels. Direct microscopic visualization[34,35] suggests that texture length scales should be much smaller than sample thickness under shear flow conditions expected in these experiments, providing an appropriate mechanism for averaging over the distribution of director orientation as the light beam passes through tens or even hundreds of "domains".

Table 1. Optical Properties of Model LCP Solutions

solution	Δn_o	B (mL/g)
50 wt % HPC in water	0.0090	0.017
27 wt % HPC in *m*-cresol	0.0035	0.012
13.5 wt % PBDG in *m*-cresol	0.0054	0.038
19 wt % PBLG in *m*-cresol	0.0080	0.039

Hongladarom et al.[9] postulated that experimentally measured birefringence would be proportional to bulk orientation parameter, with a proportionality constant that would represent the maximum birefringence possible in a given solution, Δn_o, for perfect orientation (i.e., for $S = 1$). Independent measurements of orientation parameter by X-ray scattering allow determination of Δn_o for the four solutions studied here; it is simply the maximum value for each birefringence axis in Figures 5 and 6. It is furthermore reasonable to expect that Δn_o should be proportional to the concentration of rods. Birefringence under flow could then be written:

$$\Delta n = cBS \tag{6}$$

The constant B should depend only on the dielectric properties of the rodlike macromolecules and solvent and thus be constant for a given model system. Table 1 summarizes values of Δn_o and B for the four solutions studied here. The B values obtained for the two PBG solutions are in good agreement.

Despite the agreement seen here and in Figures 5 and 6, it is difficult to assess the extent to which the X-ray data collection and analysis procedures used here (typical, we believe, of other studies) lead to faithful values of the orientation parameter S. We have noted that base line subtraction procedures directly influence measured S values. Further, since it is impossible to perfectly align all the molecules, the assumption that oriented rods will give a δ function response in an azimuthal scan, implicit in the order parameter analysis, cannot be tested. Finally, the standard methods for extracting orientation parameters from X-ray scattering patterns assume axial symmetry in the orientation distribution function, which need not be present under shear flow. We feel that some measure of restraint is called for when attaching *detailed* structural significance to orientation parameters measured by these methods and are satisfied to treat all of these methods as more general, albeit quantitative, measures of orienation that are useful for studying trends with shear rate, comparing various materials, etc.

We now consider the failure of birefringence during relaxation of the more concentrated PBLG solutions. In previous relaxation studies, birefringence in several PBG solutions was seen to increase to a value comparable to that observed in a monodomain.[10] X-ray data in Figure 8a and neutron scattering data of Walker and Wagner[16] show that this genuinely reflects increasing bulk molecular alignment in at least *some* cases. However, the results of Figure 8b raise the question of how large birefringence and moderate orientation can be reconciled. First, we recall that the spectrographic technique is very robust in avoiding difficulties associated with high optical anisotropy, in that numerical values of birefringence are extracted from the characteristic wavelength dependence of analyzed polarized light that has experienced many orders of retardation. The raw spectra unambiguously reflect a large phase

shift introduced between orthogonal components of the light polarization vector. We hypothesize that this failure is a breakdown of the presumed *relationship* between birefringence and bulk orientation rather than a failure of the spectrographic technique, *per se*.

As discussed above, birefringence measurements of orientation are predicated by the assumption that a sufficient number of "domains" is sampled along a light path to effectively average the optical properties over the distribution of domain orientations. Evidentally, this condition is met under steady shear flow conditions. During relaxation, however, it is well known that LCP solutions often exhibit formation of specific larger scale structures ("bands"), as well as a more general coarsening of the texture. One manifestation is an increase in depolarization effects during relaxation,[10] since less efficient averaging of optical properties *along* the light path leads to greater variability in effective optical properties among *neighboring* light paths. Hongladarom and Burghardt observed that these effects were quite severe in 20 wt % solutions of PBG (see, for instance, Figure 7 of reference 10). Indeed, the polarization becomes so mixed that extraction of birefringence values is impossible during a portion of the relaxation. This accounts for the gap in birefringence data in Figure 8b. If texture coarsens to the point where depolarization effects hinder birefringence measurements, it is plausible that there is no longer effective averaging of the domain distribution function along light paths, compromising the relationship between birefringence and bulk orientation. Under these circumstances, it appears that the measured birefringence value reflects the *local* degree of order, S_m, but not the misalignment of domains on larger length scales, $\bar{S}$.

Comparing these methods in broader terms, the failure of birefringence during relaxation for one solution suggests that this technique requires caution in application. Fortunately, this failure appears to be closely associated with extreme depolarization, which could prove useful as a self-diagnosis to avoid situations where the connection between birefringence and bulk orientation is compromised. Given this caveat, birefringence is still attractive in light of its comparative simplicity and low cost, particularly with respect to transient measurements. In addition, experiments probing alternate projections of the orientation state are comparatively easy.[12] Increasing availability of X-ray area detectors and high flux sources means that X-ray scattering measurements are approaching a comparable level of convenience.[5] Neutron scattering offers the advantage of mature procedures for absolute calibration of scattering intensity in 2-D measurements, but will likely remain limited by comparatively slow data acquisition and the need for deuteration to achieve appreciable scattering contrast. Both scattering methods both offer the significant advantage that they may be applied to opaque materials.

5. Conclusions

Measurements of molecular orientation in four LCP solutions using flow birefringence, X-ray scattering, and neutron scattering generally show self-consistency. In steady shear flow, flow birefringence is seen to be directly proportional to orientation parameters measured by X-ray scattering. In PBG/cresol solutions of different composition, the birefringence is also proportional to concentration. A 19 wt % solution of PBLG in *m*-cresol was studied by all three techniques, which consistently showed the persistence of moderate orientation at low shear rates, unlike other recent neutron data showing low orientation at low shear rates in PBLG solutions in different solvents.[15,21]

Flow birefringence failed to accurately reflect bulk molecular orientation during relaxation of the 19 wt % PBLG solution upon cessation of shear flow. Despite large increases in birefringence, X-ray and neutron scattering data showed only modest changes in orientation. It was hypothesized that texture coarsening during relaxation compromised the relationship between birefringence and bulk orientation due to inadequate sampling of the distribution of domain orientations along the light path. The failure was accompanied by strong depolarization effects in the birefringence measurements that can serve as a warning in future experiments.

Acknowledgment. We gratefully acknowledge financial support from the NSF Materials Research Center at Northwestern University (DMR-9120521), from an NSF Young Investigator Award (CTS-9457083), and from a DuPont Young Faculty Grant. Research partially supported by the Division of Materials Sciences, U.S. Department of Energy, under contract number DE-AC05-96OR22464 with Lockheed Martin Energy Research Corp. Financial support for P.D.B. was provided by the Oak Ridge Institute for Science and Education, while V.M.U. was supported by an NSF Graduate Fellowship. Some of the birefringence data were collected by Melissa Mahoney and Scott Norquist. We wish to thank Dr. Steven Ehrlich for assistance with the X-ray scattering experiments at Brookhaven. The HPC used in the aqueous solution was supplied by Prof. Nino Grizzuiti.

References and Notes

(1) Marrucci, G.; Greco, F. *Adv. Chem. Phys.* **1993**, *86*, 331.
(2) Picken, S. J.; Aerts, J.; Visser, R.; Northolt, M. G. *Macromolecules* **1990**, *23*, 3849.
(3) Picken, S. J.; Aerts, J.; Doppert, H. L.; Reuvers, A. J.; Northolt, M. G. *Macromolecules* **1991**, *24*, 1366.
(4) Keates, P.; Mitchell, G. R.; Peuvrel-Disdier, E.; Navard, P. *Polymer* **1993**, *34*, 1316.
(5) Keates, P.; Mitchell, G. R.; Peuvrel-Disdier, E.; Riti, J. B.; Navard, P. *J. Non-Newtonian Fluid Mech.* **1994**, *52*, 197.
(6) Odell, J. A.; Ungar, G.; Feijoo, J. L. *J. Polym. Sci.: Part B: Polym. Phys.* **1993**, *31*, 141.
(7) Radler, M. J.; Landes, B. G.; Nolan, S. J.; Broomall, C. F.; Chritz, T. C.; Rudolf, P. R.; Mills, M. E.; Bubeck, R. A. *J. Polym. Sci.: Part B: Polym. Phys.* **1994**, *32*, 2567.
(8) Chow, A. D.; Hamlin, R. D.; Ylitalo, C. *Macromolecules* **1992**, *25*, 7135.
(9) Hongladarom, K.; Burghardt, W. R.; Baek, S. G.; Cementwala, S.; Magda, J. J. *Macromolecules* **1993**, *26*, 772.
(10) Hongladarom, K.; Burghardt, W. R. *Macromolecules* **1993**, *26*, 785.
(11) Hongladarom, K.; Secakusuma, V.; Burghardt, W. R. *J. Rheol.* **1994**, *38*, 1505.
(12) Hongladarom, K.; Burghardt, W. R. *Macromolecules* **1994,** *27*, 483.
(13) Burghardt, W.; Bedford, B.; Hongladarom, K.; Mahoney, M. In *Flow-Induced Structure in Polymers*; Nakatani, A. I., Dadmun, M. D., Eds., ACS Symposium Series 597, American Chemical Society: Washington, D.C., 1995, p 308.
(14) Bedford, B. D.; Burghardt, W. R. *J. Rheol.* **1994**, *38*, 1657.
(15) Dadmun, M. D.; Han, C. C. *Macromolecules* **1994**, *27*, 7522.
(16) Walker, L. M.; Wagner, N. J. *Macromolecules* **1996**, *29*, 2298.
(17) Dadmun, M. D. In *Flow-Induced Structure in Polymers*; Nakatani, A. I., Dadmun, M. D., Eds., ACS Symposium Series 597, American Chemical Society: Washington, D.C., 1995, p 320.
(18) Larson, R. G.; Doi, M. *J. Rheol.* **1991**, *35*, 539.
(19) Walker, L. M.; Wagner, N. J. *Macromolecules* **1994**, *27*, 5979.

(20) Burghardt, W. R.; Hongladarom, K. *Macromolecules* **1994**, *27*, 2327.
(21) Walker, L. M. Ph.D. Dissertation, University of Delaware, 1995.
(22) Guido, S.; Grizzutti, N. *Rheol. Acta* **1995**, *34*, 137.
(23) Bedford, B. D.; Burghardt, W. R. *J. Rheol.* **1996**, *40*,235.
(24) Koehler, W. C. *Physica* **1986**, *137B*, 320.
(25) Wignall, G. D.; Bates, F. S. *J. Appl. Crystallogr.* **1987**, *20*, 28.
(26) Higgins, J. S.; Benoit, H. C. *Polymers and Neutron Scattering*; Oxford: New York, 1994.
(27) Baltá-Calleja, F. J.; Vonk, C. B. *X-ray Scattering of Synthetic Polymers*; Elsevier: Amsterdam, 1989.
(28) Mitchell, G. R.; Windle, A. H. In *Developments in Crystalline Polymers* - 2; Bassett, D. C., Ed.; Elsevier: London, 1988; Chapter 3.
(29) Walker, L.; Wagner, N. *J. Rheol.* **1994**, *38*, 1525.
(30) Walker, L. M.; Wagner, N. J.; Larson, R. G.; Mirau, P. A.; Moldenaers, P. *J. Rheol.* **1995**, *39*, 925.
(31) Mewis, J.; Moldenaers, P. *Mol. Cryst. Liq. Cryst.* **1987**, *153*, 291.
(32) Moldenaers, P.; Mewis, J. *J. Rheol.* **1986**, *30*, 567.
(33) Larson, R. G.; Mead, D. W. *J. Rheol.* **1989**, *33*, 1251.
(34) Larson, R. B.; Mead, D. W. *Liq. Cryst.* **1992**, *12*, 751.
(35) Larson, R. G.; Mead, D. W. *Liq. Cryst.* **1993**, *15*, 151.

MA960171H